Acta Crystallographica Section B
Structural Science
ISSN 0108-7681

Variable-temperature neutron diffraction studies of the short, strong N···O hydrogen bonds in the 1:2 co-crystal of benzene-1,2,4,5-tetracarboxylic acid and 4,4′-bipyridyl

John A. Cowan,[a,b]*‡ Judith A. K. Howard,[b] Garry J. McIntyre,[a] Samuel M.-F. Lo[c] and Ian D. Williams[c]

[a]Institut Laue–Langevin, 6 rue Jules Horowitz, BP156, 38042 Grenoble CEDEX 9, France, [b]Department of Chemistry, University of Durham, Durham DH1 3LE, England, and [c]Department of Chemistry, Hong Kong University of Science and Technology, Clear Water Bay, Hong Kong, People's Republic of China

‡ Current Address: Intense Pulsed Neutron Source, Argonne National Laboratory, 9700 South Cass Avenue, Argonne, IL 60439, USA.

Correspondence e-mail: jacowan@anl.gov

Received 8 August 2003
Accepted 30 October 2003

The 1:2 adduct of benzene-1,2,4,5-tetracarboxylic acid and 4,4′-bipyridyl at 100 K has been studied by single-crystal neutron diffraction at 20, 200 and 296 K. The structure contains two short, strong N···O hydrogen bonds: one O—H···N hydrogen bond [O···N 2.6104 (17) Å at 20 K] and one short N—H···O hydrogen bond [N···O 2.5220 (17) Å at 20 K]. The N—H distance in the N—H···O hydrogen bond changes from 1.207 (3) Å at 20 K to 1.302 (4) Å at 296 K and the N···O distance increases to 2.5315 (16) Å at 296 K. At 200 K the H atom lies in an intermediate position 1.251 (6) Å from the N atom with an N···O separation of 2.520 (4) Å. The O—H···N hydrogen bond, on the other hand, does not change with temperature.

1. Introduction

Intermolecular O—H···O hydrogen bonds have been studied extensively by neutron diffraction and there are many studies in which the proton position has been found to be approximately equidistant from the O atoms (Wilson, 2000). There are, however, relatively few neutron diffraction studies of very short N···O hydrogen bonds (Steiner *et al.*, 2000). The shortest such hydrogen bond studied by neutron diffraction so far occurs in the crystal structure of 4-methylpyridine and pentachlorophenol (Steiner *et al.*, 2001) with an N···O separation in the hydrogen bond of 2.506 (3) Å at 20 K. In this hydrogen bond the H atom lies approximately equidistant from the N and O atoms, and is observed to change position with changing temperature; at 20 K the proton lies closer to the N atom and at 300 K it lies closer to the O atom. Similar temperature-dependent proton migration has also been observed in the short O—H···O hydrogen bond in urea–phosphoric acid (Wilson, 2001), where the H atom moves from an asymmetric position at 150 K to a centred position at 300 K.

The X-ray crystal structure of the 1:2 adduct of benzene-1,2,4,5-tetracarboxylic acid (BTA) and 4,4′-bipyridyl (BPY) has recently been published by Lough *et al.* (2000) and contains two short N···O hydrogen bonds. One of the hydrogen bonds appears to be a short O—H···N hydrogen bond with the H atom close to the O atom [O···N 2.613 (2) Å and O—H 0.84 Å]. The other bond is much shorter and the H atom has been placed approximately in the centre of the hydrogen bond [N···O 2.521 (2) and N—H 1.22 (2) Å]. In the O—H···H hydrogen bond the H atom was refined as riding on the O atom, in the N—H···O hydrogen bond the hydrogen atom was refined freely. To determine accurately the H-atom

© 2003 International Union of Crystallography
Printed in Great Britain – all rights reserved

positions and to reliably observe any temperature-dependent changes in the hydrogen bonds, neutron diffraction experiments are essential. To this end, we have collected neutron diffraction data at 296, 200 and 20 K. Complementary X-ray diffraction data have also been collected at 30 K.

2. Experimental

2.1. Synthesis

Crystals were formed in ≥80% yield by heating BPY and BTA in a 2:1 ratio (2:1 mmol) in 1 mL of H_2O for 2 d at 453 K in a 23 mL Teflon-lined Parr vessel under autogenous pressure. Phase purity was established by powder X-ray diffraction and elemental analysis. A typical crystal size was 1–2 mm^3. Larger specimens up to 5 mm^3 could be obtained by cyclic heating and cooling of the bombs between 373–453 K.

2.2. Neutron data collection

Neutron diffraction data were collected on the diffractometer D19 at the Institut Laue–Langevin (ILL) at 20 and 296 K, and on the Laue diffractometer LADI (Wilkinson & Lehmann, 1991; Cipriani *et al.*, 1994) at 200 K.

In the D19 experiment a crystal of volume ∼5 mm^3 was attached with epoxy glue to a vanadium pin, which was then mounted upon the Displex cryorefrigerator (Archer & Lehmann, 1986) on the χ circle of D19. D19 was equipped with a large ($4 \times 64^\circ$) multiwire proportional ^{3}He-gas area detector (Thomas *et al.*, 1983), which for this experiment allowed the collection of several reflections simultaneously, optimum delineation of each reflection from the considerable background due mainly to the incoherent scattering from hydrogen in the sample, and very precise determination of the lattice parameters since the centres of all the reasonably strong reflections were observed. Diffraction data were collected in normal-beam geometry at room temperature with a wavelength of 1.3018 (1) Å from a Ge(115) monochromator. Two test reflections ($\bar{2}00$ and $6\bar{6}0$) were measured approximately every 50 reflections and these showed no significant change during the data collection.

After half of the allocated neutron beam-time, at which time the room-temperature data collection was 81% complete to $\sin\theta/\lambda = 0.63$ Å^{-1}, the crystal was cooled to 20 K at 2 K min^{-1} while monitoring the strong $\bar{2}00$ reflection. Data were collected at 20 K in the same manner.

Cell dimensions were refined using the ILL program *RAFD*19 and integrated intensities produced using the ILL program *RETREAT* (Wilkinson *et al.*, 1988). The data were corrected for absorption in the crystal using the ILL program *D*19*ABS*), which is based on the *CCSL* suite (Matthewman *et al.*, 1982). The low-temperature data were also corrected for absorption by the aluminium and vanadium cryorefrigerator vacuum and heat shields (maximum transmission 0.892, minimum transmission 0.602).

An opportunity arose to use the neutron Laue diffractometer LADI (Wilkinson & Lehman, 1991; Cipriani *et al.*, 1994) during trials of this diffractometer on a thermal beam. LADI is normally installed on a cold-neutron beam for macromolecular crystallography, but has been proven to be very well suited to small-molecule crystallography if located on a thermal beam (Myles *et al.*, 1998; Cole *et al.*, 2001).

A smaller crystal of volume ∼0.1 mm^3 from a separate synthetic batch was mounted using an identical pin upon an Edwards cryorefrigerator on LADI and cooled to 200 K, where data were collected. There were 15 Laue diffraction patterns obtained with the crystal bathed in the non-monochromated thermal neutron beam, and rotated 20° around the axis of the cylindrical detector between the 2 h exposures. The patterns were indexed using *LAUEGEN* (Campbell, 1995) and the reflections integrated using a modified version of the *RETREAT* program for two dimensions (Wilkinson *et al.*, 1988). The absolute magnitudes of the cell dimensions cannot be measured accurately by Laue diffraction, only the relative magnitudes and the cell angles. For this reason, and because of possible distortions in the shape of the area detector and possible miscentring of the crystal, the cell dimensions used in the data processing have not been used in the refinements. The 200 K cell dimensions were estimated by the least-squares fit of a straight line to the previously collected neutron and X-ray data, and assigned slightly exaggerated s.u.s considering the assumptions made. The data were normalized for the incident spectrum by comparison of repeated and equivalent reflections with *LAUENORM* (Campbell *et al.*, 1996); only reflections with wavelengths between 1.1 and 1.9 Å were accepted in this step. In all, 13 172 reflections were measured, 6367 with λ between 1.1–1.9 Å, to yield 1961 unique reflections. Owing to the regular form of the crystal, the attenuation owing to absorption would be nearly constant for all reflections observed at the same wavelength, and variation of the attenuation with wavelength would be corrected in the empirical normalization over wavelength. Therefore, no explicit correction for absorption was made.

2.3. X-ray data collection

X-ray diffraction data were collected at 30 K on a Bruker SMART-CCD diffractometer (Bruker, 1998) with graphite-monochromated Mo $K\alpha$ radiation. The crystal was cooled using an Oxford Cryosystems HeliX helium-flow device (Goeta *et al.*, 1999) to 30 K, the minimum reliable temperature attainable, for data collection. Data were also collected at 100 K and room temperature to measure the changes in the cell dimensions.

2.4. Structural refinements

The X-ray structure was solved using direct methods using the program *SHELXS* (Sheldrick, 1990) and refined by full-matrix least-squares on F^2 using *SHELXL* (Sheldrick, 1997). The structure was consistent with the solution obtained by Lough *et al.* (2000). Anisotropic displacement parameters were refined for all non-H atoms. All the H atoms were found in the difference-Fourier maps and refined with isotropic displacement parameters. The C—H distances [C—H 0.938 (15)–0.990 (15) Å] all refined to within standard ranges,

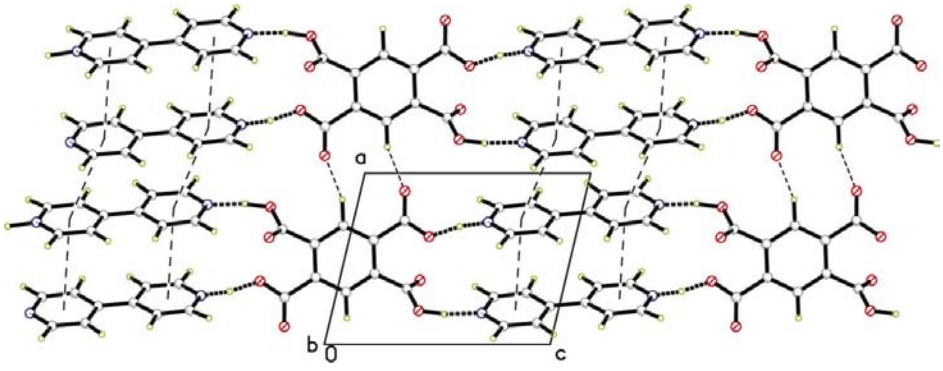

Figure 1
Packing diagram viewed parallel to the *b* axis, illustrating the chains of molecules along the [01$\bar{2}$] direction. The heavy dashed lines indicate N···O hydrogen bonds, the thin dashed lines indicate π–π interactions and C—H···O hydrogen bonds. The columns of BPY and BTA molecules are clearly seen.

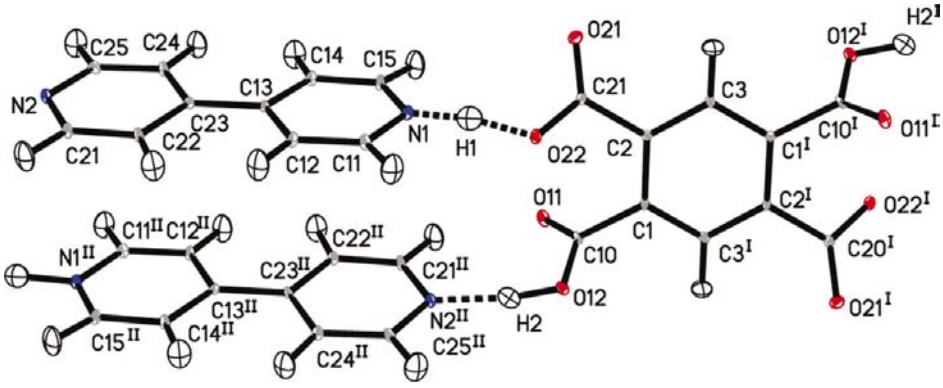

Figure 2
Displacement ellipsoid plot (at the 50% probability level) from the 20 K neutron data. Only the H atoms of interest, H1 and H2, are labelled. Hydrogen bonds are indicated by the dashed lines. [Symmetry codes: (I) $1-x, 1-y, -z$; (II) $1-x, 2-y, -2-z$.]

allowing for the artificial contraction in X-ray data (Allen *et al.*, 1992) and there were no anomalous values of U_{iso}. As we were interested in the behaviour of the H atoms and the data were collected at such low temperature, it would be artificial to apply any constraints to the stable and converged refinement.

The initial structural model for all three neutron refinements (295, 200 and 20 K) was taken from the X-ray diffraction results. The structures were refined using *SHELXL* (Sheldrick, 1997) with full-matrix least-squares on F^2 using the neutron-scattering lengths tabulated by Sears (1992). All atoms were refined with anisotropic displacement parameters. Thermal-motion analysis in *PLATON* (Spek, 1990) estimated the apparent foreshortening of the bond lengths owing to libration to be approximately 0.0002 Å and consequently no librational correction has been applied to the bond lengths. Molecular graphics were produced using *SHELTX/PC* (Sheldrick, 1999). The data collections and refinement details are summarized in Table 1.[1]

[1] Supplementary data for this paper are available from the IUCr electronic archives (Reference: BS5001). Services for accessing these data are described at the back of the journal.

3. Results and discussion

3.1. Structures

The structure has been discussed in detail by Lough *et al.* (2000). Unless otherwise specified, all parameters for discussion herein are taken from the 20 K neutron data. In summary, two independent N···O hydrogen bonds link the BPY and BTA molecules in a one-dimensional chain along the [01$\bar{2}$] direction (Fig. 1). The BPY molecules form π–π stacked columns parallel to the *a* axis; the BTA molecules form parallel columns stacked edge-to-edge and linked by a weak C—H···O hydrogen bond. C—H···O and C—H···π hydrogen bonds link the chains of molecules in the *bc* plane.

The O12—H2···N2 hydrogen bond (Table 2*a*) is clearly an ordered O—H···N hydrogen bond. This hydrogen bond and the auxiliary C—H···O hydrogen bond (C21—H21···O11) form a common synthon observed between carboxylic acid groups and BPY (Shan *et al.*, 2002). There is no evidence of disorder in the anisotropic displacement parameters (Fig. 2) of the proton, which has a U_{eq} value of 0.0178 (6) Å^2 compared with an average of 0.0224 Å^2, with an average s.u. of 7×10^{-4} for the bipyridyl H atoms, or in the difference-Fourier map (Fig. 3*a*). The C—O bond lengths in the carboxylic acid group [C10—O11 1.219 (2) and C10—O12 1.312 (2) Å] agree with those tabulated in the *International Tables for Crystallography* (Allen *et al.*, 1992) for a carboxylic acid group attached to a phenyl ring of 1.305 (20) and 1.226 (20) Å. The C—N—C bond angles for BPY molecules in the Cambridge Structural Database (Allen, 2002) are 121.4 (9) and 116.3 (16)° for a protonated and an unprotonated molecule, respectively. The C21—N2—C25 angle of 118.2 (1)° favours the unprotonated conformation, although the size of the s.u.'s prevents any firm conclusions being drawn from this comparison.

The N1···H1···O22 hydrogen bond (Table 2*b*) is quite different and unusual, even though it occurs between the same chemical groups in a very similar intermolecular environment to the O12—H2···N2 hydrogen bond. At 20 K the proton lies close to the centre of the hydrogen bond. The C—O bond lengths [C20—O21 1.235 (2), C20—O22 1.2845 (19) Å] in the carboxylate group have been significantly modified by the hydrogen bond. They lie as a compromise between the expected carboxylic acid values (see above) and the value expected for a carboxylate group [1.255 (10) Å, *International*

Table 1
Experimental details.

	20 K	296 K	200 K†	30 K
Crystal data				
Chemical formula	$C_{10}H_8O_8{\cdot}2C_{10}H_8N_2$	$C_{10}H_8O_8{\cdot}2C_{10}H_8N_2$	$C_{10}H_8O_8{\cdot}2C_{10}H_8N_2$	$C_{10}H_8O_8{\cdot}2C_{10}H_8N_2$
M_r	566.00	566.00	566.00	566.52
Cell setting, space group	Triclinic, $P\bar{1}$	Triclinic, $P\bar{1}$	Triclinic, $P\bar{1}$	Triclinic, $P\bar{1}$
a, b, c (Å)	7.3561 (2), 9.5856 (2), 10.1478 (3)	7.5011 (2), 9.7868 (3), 10.2303 (3)	7.541 (1), 9.715 (1), 10.204 (1)	7.357 (2), 9.587 (3), 10.147 (3)
α, β, γ (°)	65.203 (2), 72.699 (3), 77.099 (3)	64.140 (3), 71.682 (3), 75.516 (3)	64.51 (1), 72.03 (1), 76.08 (1)	65.256 (4), 72.687 (4), 77.052 (4)
V (Å^3)	616.16 (3)	635.93 (4)	635.9 (5)	616.4 (3)
Z	1	1	1	1
D_x (Mg m^{-3})	1.525	1.478	1.478	1.526
Radiation type	Neutron	Neutron	Neutron	Mo $K\alpha$
No. of reflections for cell parameters	2325	2509	N/A	1690
θ range (°)	5–55	3–55	N/A	12.0–27.7
μ (mm^{-1})	0.17	0.17	0.00	0.11
Temperature (K)	20 (2)	293 (2)	200 (2)	30 (2)
Crystal form, colour	Prism, colourless	Prism, colourless	Plate, colourless	Block, colourless
Crystal size (mm)	4.5 × 1.2 × 0.75	4.5 × 1.2 × 0.75	1.3 × 0.6 × 0.2	0.5 × 0.35 × 0.15
Data collection				
Diffractometer	D19	D19	LADI Laue diffractometer	Bruker SMART-CCD
Data collection method	ω scans	ω scans	Laue method	ω scans
Absorption correction	Gaussian	Gaussian	None	None
T_{min}	0.602	0.602	–	–
T_{max}	0.892	0.892	–	–
No. of measured, independent and observed reflections	2464, 1866, 1743	2914, 2145, 1894	1961, 1961, 1192	5958, 2549, 2126
Criterion for observed reflections	$I > 2\sigma(I)$	$I > 2\sigma(I)$	$I > 2\sigma(I)$	$I > 2\sigma(I)$
R_{int}	0.023	0.028	0.113	0.038
θ_{max} (°)	56.3	55.5	30.7	27.6
Range of h, k, l	$-9 \Rightarrow h \Rightarrow 9$ $-12 \Rightarrow k \Rightarrow 6$ $-12 \Rightarrow l \Rightarrow 12$	$-9 \Rightarrow h \Rightarrow 9$ $-12 \Rightarrow k \Rightarrow 4$ $-12 \Rightarrow l \Rightarrow 12$	$-7 \Rightarrow h \Rightarrow 7$ $-12 \Rightarrow k \Rightarrow 13$ $0 \Rightarrow l \Rightarrow 14$	$-9 \Rightarrow h \Rightarrow 9$ $-12 \Rightarrow k \Rightarrow 12$ $-12 \Rightarrow l \Rightarrow 12$
No. and frequency of standard reflections	2 every 75 reflections	2 every 70 reflections	–	–
Refinement				
Refinement on	F^2	F^2	F^2	F^2
$R[F^2 > 2\sigma(F^2)]$, $wR(F^2)$, S	0.033, 0.086, 1.16	0.035, 0.088, 1.05	0.052, 0.125, 1.28	0.034, 0.089, 1.66
No. of reflections	1866	2145	1961	2549
No. of parameters	290	291	289	235
H-atom treatment	Refined independently	Refined independently	Refined independently	Refined independently
Weighting scheme	$w = 1/[\sigma^2(F_o^2) + (0.0471P)^2 + 1.8319P]$, where $P = (F_o^2 + 2F_c^2)/3$	$w = 1/[\sigma^2(F_o^2) + (0.0417P)^2 + 1.6198P]$, where $P = (F_o^2 + 2F_c^2)/3$	$w = 1/[\sigma^2(F_o^2) + (0.050P)^2]$, where $P = (F_o^2 + 2F_c^2)/3$	$w = 1/[\sigma^2(F_o^2) + (0.030P)^2]$, where $P = (F_o^2 + 2F_c^2)/3$
$(\Delta/\sigma)_{max}$	0.001	0.023	<0.0001	<0.0001
$\Delta\rho_{max}$, $\Delta\rho_{min}$ (e Å^{-3})	0.52, −0.57	0.43, −0.43	0.71, −0.75	0.35, −0.23
Extinction method	*SHELXL*	*SHELXL*	None	*SHELXL*
Extinction coefficient	0.0052 (5)	0.0066 (6)	–	0.013 (3)

Computer programs used: *MAD* (Barthelemy *et al.*, 1982), *LADI Control* and *SMART* (Bruker, 1998), *RAFD19* (Filhol, 1998), *LAUEGEN* (Campbell, 1995), *SAINT* (Bruker, 1998), *RETREAT* (Wilkinson *et al.* 1988), *INTEGRATE+ and LAUENORM* (Wilkinson, *et al.* 1988), *SHELXS*97 (Sheldrick, 1990), *SHELXL*97 (Sheldrick, 1997). † The 200 K cell dimensions were estimated by a least-squares fit of a straight line to the previously collected neutron and X-ray data.

Tables for Crystallography]. The C11—N1—C15 angle of 120.2 (1)° agrees with the protonated conformation (see above), although again the size of the s.u.'s prevents any firm conclusions being drawn from this comparison. The proton position in the hydrogen bond is sharply defined. There is no evidence of disorder in the difference-Fourier map (Fig. 3*b*) or anisotropic displacement parameters (Fig. 2) and again U_{eq} for the proton [0.0209 (6) Å^2] is slightly smaller than the average for the BPY H atoms. Refinement with the proton in the hydrogen bond disordered between two positions gave unsatisfactory results.

At 296 K the O12—H2···N2 hydrogen-bond parameters are identical to those at 20 K (Table 2*a*), whereas the N1···H1···O22 hydrogen bond has changed significantly. The N—H bond length increases by 0.095 (5) Å and the H—O bond distance decreases by 0.085 (5) Å (the s.u.'s have been estimated from the measured values as $\sigma^2 = \sigma_1^2 + \sigma_2^2$), equivalent to the proton migrating ∼0.1 Å across the

Table 2
Hydrogen-bond parameters (Å, °).

	$D\cdots A$	D—H	H$\cdots A$	$D\cdots$H—A
O21—H2$\cdots$N2				
296 K	2.6095 (17)	1.078 (4)	1.542 (3)	169.6 (3)
200 K	2.609 (3)	1.061 (6)	1.556 (5)	170.5 (7)
30 K†	*2.6151 (15)*	*0.99 (2)*	*1.63 (3)*	*172 (2)*
20 K	2.6104 (17)	1.068 (3)	1.551 (3)	170.2 (3)
N1$\cdots$H1$\cdots$O22				
296 K	2.5315 (16)	1.302 (4)	1.240 (4)	169.6 (3)
200 K	2.520 (4)	1.251 (6)	1.280 (6)	169.4 (6)
30 K†	*2.5248 (14)*	*1.14 (2)*	*1.40 (2)*	*170 (2)*
20 K	2.5220 (17)	1.207 (3)	1.325 (3)	170.2 (3)

† Hydrogen position from X-ray diffraction.

Table 3
Temperature variation of distances in the weak C—H$\cdots$O hydrogen bonds.

	$D\cdots A$ (Å) – 296 K	$D\cdots A$ (Å) – 200 K	$D\cdots A$ (Å) – 20 K
C11$\cdots$O22	3.317 (2)	3.296 (4)	3.243 (2)
C12$\cdots$O21	3.278 (2)	3.252 (4)	3.231 (2)
C21$\cdots$O11	3.120 (2)	3.111 (4)	3.106 (2)
C22$\cdots$O11	3.353 (2)	3.330 (4)	3.309 (2)
C24$\cdots$O21	3.404 (2)	3.383 (4)	3.365 (2)
C25$\cdots$O12	3.4690 (19)	3.446 (4)	3.426 (2)

hydrogen bond, from closer to the N atom to become closer to the O atom. The change in the proton position is accompanied by a slight increase of the N$\cdots$O distance of 0.01 (2) Å. Again there is no evidence of disorder in the difference-Fourier map and the displacement parameters of the hydrogen-bond proton are smaller than those of the BPY H atoms [average U_{eq} for the BPY C—H H atoms = 0.0782 (12) Å^2 and U_{eq} for H1 = 0.0581 (13) Å^2]. The unit-cell volume has expanded by 3.2% from 616.16 (3) to 635.93 (4) Å^3. The greatest changes (∼1.5%) in the unit-cell edges over the temperature range occur in a and b, while the change in c is only ∼0.7%. The largest component of the strong hydrogen bonds, which have changed little in overall length, lies along the c direction. Conversely, the weaker C—H$\cdots$O hydrogen bonds have significantly increased in length (Table 3), as have the distances in the π–π interactions (Table 4); the distance between the ring centres has increased by 0.13 Å for the interaction between the molecular chains and by 0.06 Å for the interaction within the chains.

At 200 K, although the Laue experiment yields s.u.s that are larger than those for the monochromatic experiments, the observations consistent with the above can be made. The O12—H2$\cdots$N2 hydrogen bond is again identical to its 20 K configuration, while the position of the H atom in the N1$\cdots$H1$\cdots$O22 hydrogen bond is intermediate between the positions found at 296 and 20 K extremes. There is again no evidence of disorder in the difference-Fourier map and the displacement parameters of the proton in the hydrogen bond are smaller than the BPY C—H protons [average for BPY C—H protons = 0.052 (2) Å^2, U_{eq}(H1) = 0.0345 (19) Å^2].

The bond lengths and angles in the 30 K X-ray diffraction structure are not significantly different from those of the 20 K neutron structure except for those bonds involving the H atoms. The X-ray derived anisotropic displacement parameters appear to be slightly larger than the neutron parameters by a greater magnitude than can be accounted for by the temperature difference. This discrepancy is most likely due to the anisotropy of the electron cloud and the loss of electrons to the bonding density, but could also be caused by extinction in the neutron data (which reduces the intensity of the low-angle data), thermal diffuse scattering or inaccuracies in the absorption correction. The X-ray difference-Fourier

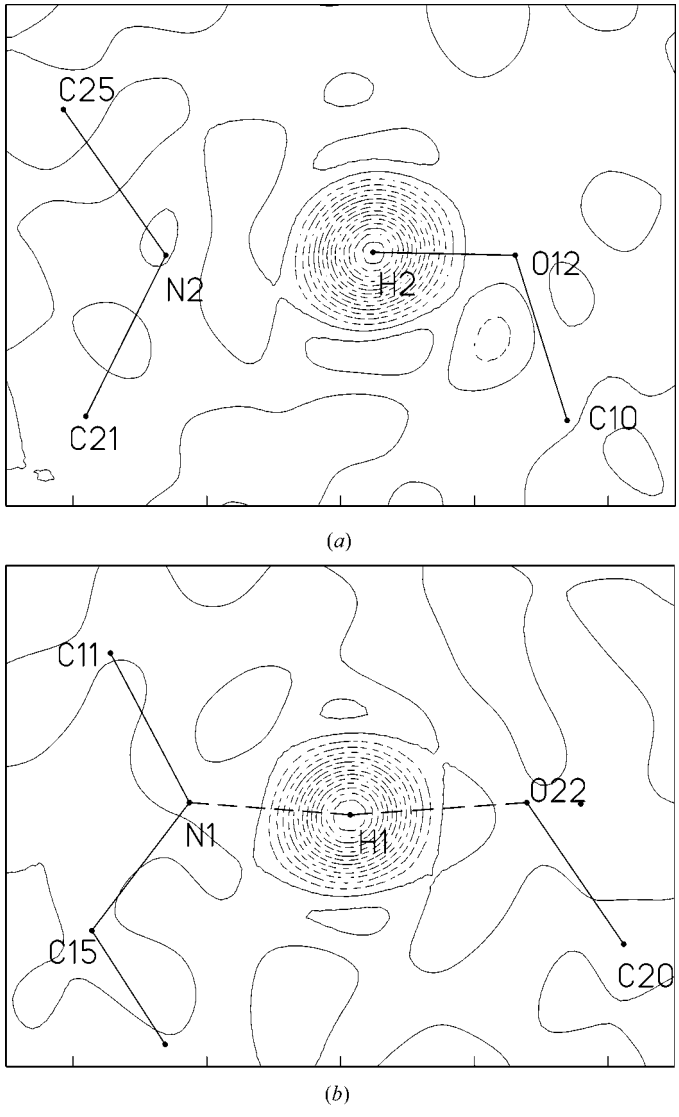

Figure 3
Difference-Fourier map calculated from the 20 K neutron diffraction data with H2 (Fig. 3*a*) or H1 (Fig. 3*b*) omitted from the model. The contours are at a nuclear scattering density of 1 fm Å^{-3} and dashed lines indicate negative contours. The neutron scattering length of hydrogen is negative, and therefore the residual scattering length density appears as a 'hole' in the difference-Fourier map. The residual nuclear density is localized on the H-atom position and there is no evidence of disorder.

Table 4
Temperature variation of distances in π–π interactions.

	Centre···Centre (Å) – 296 K	Centre···Centre (Å) – 200 K	Centre···Centre (Å) – 20 K
Ring1···Ring2^{i}	3.8057 (14)	3.792 (3)	3.7449 (11)
Ring1···Ring2^{ii}	3.8730 (15)	3.799 (2)	3.7451 (11)

Ring1 = N1, C11, C12, C13, C14, C15; Ring2 = N2, C21, C22, C23, C24, C25. Symmetry codes: (i) $1-x, 2-y, -2-z$; (ii) $-x, 2-y, 2-z$.

maps calculated along the N2—O12 (Fig. 4*a*) and N1—O22 (Fig. 4*b*) hydrogen bonds with the relevant H atoms omitted cannot be used to rule out disorder in the H-atom positions.

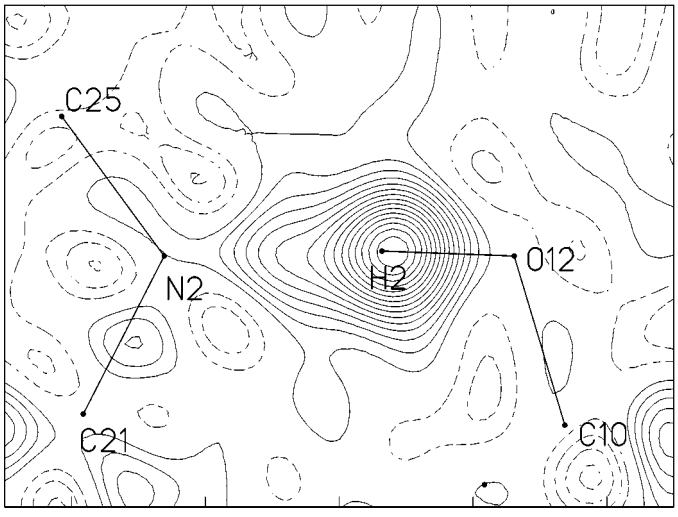

(*a*)

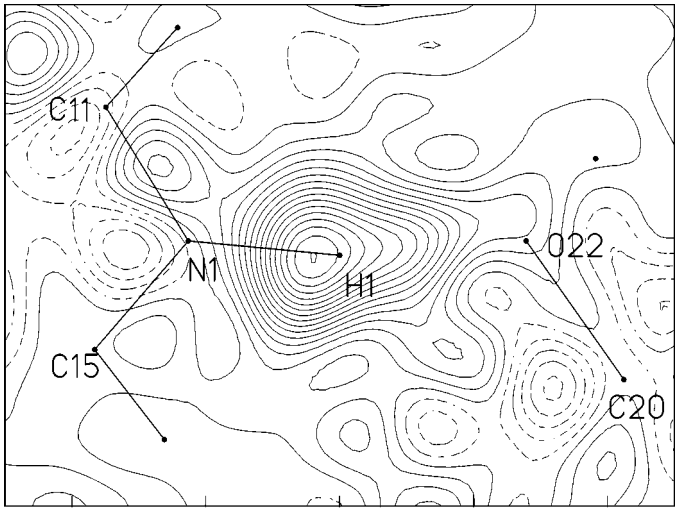

(*b*)

Figure 4
Difference-Fourier map calculated from the 30 K X-ray data with H2 (Fig. 4*a*) or H1 (Fig. 4*b*) omitted from the model. The marked positions for H1 and H2 are those from the X-ray refinement. The contours are at 0.05 e Å^{-3} and dashed lines indicate negative contours. The residual electron density in both hydrogen bonds is extended along the N—O vector and disorder of the proton positions cannot be ruled out.

3.2. Proton migration in hydrogen bonds

There are two quite different hydrogen bonds between identical chemical groups, in similar intermolecular environments. In the co-crystal of thiodiglycolic acid and BPY (Pedireddi *et al.*, 1998), two BPY and two thiodiglycolic acid molecules form a hydrogen-bonded ring that is extremely similar to that observed in this structure (Fig. 5). The thiodiglycolic acid molecules are bidentate, instead of quadradentate as for BTA, and therefore infinite one-dimensional hydrogen bonded chains cannot be formed. If weak C—H···O interactions, which connect two thiodiglycolic acid molecules into a supramolecule, are taken into account, the two structures can be considered to be isostructural. However, the strong hydrogen bonds in the thiodiglycolic BPY structure are both ordered O—H···N hydrogen bonds (O···N = 2.61 and 2.63 Å), each is assisted by a parallel C—H···O hydrogen bond (C···O = 2.94 and 3.04 Å) to form an identical motif to the O12—H2···N2 hydrogen bond in the present structure; no N—H···O hydrogen bond is formed.

The shortest N—H···O and O—H···N hydrogen bonds studied so far by neutron diffraction occur in co-crystals of methylpyridines and pentachlorophenol; the O—H···N hydrogen bond occurs in the co-crystal with 2-methylpyridine [Steiner *et al.*, 2000; N···O = 2.588 (3) Å] and the N—H···O hydrogen bond occurs in the co-crystal with 4-methylpyridine [Steiner *et al.*, 2001; N···O = 2.506 (2) Å at 20 K]. Both these hydrogen bonds are marginally shorter than those observed in the present structure, but both show similar properties.

The O—H bond length in the short O—H···N hydrogen bond in the co-crystal of 2-methylpyridine and pentachlorophenol [O—H = 1.068 (7) Å; Steiner *et al.*, 2000] has been elongated to the same extent as the O12—H2 bond [1.068 (3) Å]. As pointed out by Steiner *et al.* (2000), this elongation is much greater than the O—H extension observed in other structures and suggests that there is significant covalent character in the N···H part of the bond, as they were calculated using the bond-valence model (Brown, 1992; Steiner, 1998). This covalency can also be inferred in the present structure from the extension of the difference-Fourier

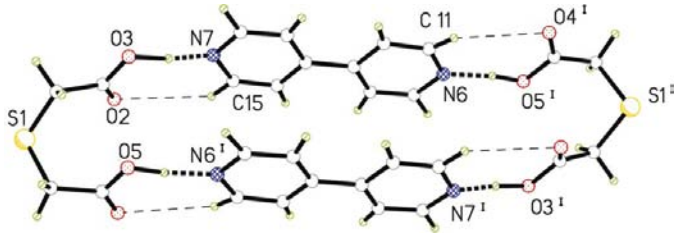

Figure 5
The hydrogen-bonded rings observed in the 1:1 co-crystal of BPY and thiodiglycolic acid (Pedireddi *et al.*, 1998). The atom names correspond to those in the Cambridge Structural Database; symmetry related atoms are indicated with a superscript I.

density along the N···O bond (Fig. 3*a*). The apparent slight extension of the O12—H2 bond length on increasing the temperature from 20 to 296 K [1.068 (3) Å at 20 K, 1.078 (4) Å at 296 K] may be because of the increased anisotropic thermal motion of the H atom. However, the change is within experimental error, which is a more likely explanation considering that no significant change is seen in the N···O distance.

The N1···H1···O22 hydrogen bond is only 0.02 Å longer than that observed in pentachlorophenol and 4-methylpyridine at 20 K for which a similar temperature-dependent proton migration is observed. In that structure, as the proton moves from 1.206 (6) Å from the N atom at 20 K to 1.306 (11) Å at 200 K, the N···O distance changes from 2.506 (2) Å at 20 K to 2.525 (4) Å at 200 K, similar to the 0.01 (2) Å increase in the N···O distance observed in the present structure.

The approximately equal *X*—H bond lengths in the hydrogen bond mean that there is significant covalent character in both the N—H and O—H bonds in the present structure. This can be seen in the X-ray diffraction difference-Fourier map (Fig. 4*b*), which also suggests that at low temperature there is more electron density in the N—H bond than in the O—H bond.

One possible explanation for the observed changes in the N1···H1···O22 hydrogen bond is that there is disorder between an N—H···O and an O—H···N hydrogen bond, with the two proton positions close together near the centre of the hydrogen bond. The relative occupancies of the two possibilities would change with temperature to create the illusion of the change in the position of H1. However, there is no evidence for this kind of disorder in the difference-Fourier maps and the displacement ellipsoid of H1. The displacement ellipsoid of O22 would also be expected to be an unusual shape to take into account the change between the different states of the carboxylic acid/carboxylate group.

It is conceivable that a static hydrogen-bond potential-energy well may be able to explain the observed results. If the potential well has an asymmetric double minimum with a low-barrier (Jeffrey, 1997), then at low temperatures the proton will only occupy the lowest possible state in the well, which must lie close to the N atom. The shape of the potential-energy well may be such that the first excited state may lie closer to the O atom and as the temperature rises, and this state becomes more populated, the expectation value of the H atom would move along the hydrogen bond. The potential well must be sufficiently broad so that the first excited state may become populated at thermal temperatures. The stretching frequencies typically observed in hydrogen bonds are of the order of $\sim$1700–3700 cm^{-1} (Jeffrey, 1997), corresponding to a temperature of $\sim$1100–2500 K. It therefore seems unlikely that the hydrogen-bond potential-energy well has changed enough to allow population of the first excited state at temperatures below 300 K.

These changes in the overall hydrogen-bond length suggest that the change in proton position is accompanied by a change in the hydrogen-bond potential-energy well, from an asymmetric well with the minimum closer to the nitrogen at 20 K to an asymmetric potential well with the minimum closer to the O atom at 296 K. This also agrees with the small change observed in the C11—N1—C15 bond angle, corresponding to changes in the bonding in the C—N and N—H bonds.

4. Conclusions

It is a remarkable demonstration of the small change necessary to convert an O—H···N hydrogen bond into a N—H···O hydrogen bond that it is sufficient to change the substitution position of the methylpyridine in the co-crystals of methylpyridine and pentachlorophenol. Of course, this change also significantly changes the intermolecular interactions. It is even more remarkable that both types of hydrogen bond occur in the same crystal between the same constituents in very similar intermolecular environments. It is not clear what causes the difference between the two hydrogen bonds or what causes the temperature-dependent proton migration. Diffraction experiments on deuterated and partially deuterated samples, spectroscopic studies and quantum-mechanical calculations will be performed to gain further insight to these problems.

A temperature-dependent phase transition observed in the co-crystal of BPY and squaric acid (Reetz *et al.*, 1994) is postulated to be due to proton transfer. Although the hydrogen bonds are significantly longer [N···O 2.613 (3) and 2.602 (3) Å] than the hydrogen bonds in which proton migration has been observed, the same mechanism may be responsible. The conversion of a long hydrogen bond to a short low-barrier hydrogen bond, accompanied by partial proton transfer, has been postulated to be an important factor in stabilizing the intermediate state in certain mechanisms of enzymatic catalysis (Cleland & Kreevoy, 1994; Hibbert & Emsley, 1990). A model that can be used to describe accurately the proton transfer in these molecular systems would also be extremely valuable in this discussion.

As also demonstrated elsewhere (Cole *et al.*, 2001) the Laue diffractometer, LADI, is very effective for fast neutron data collections on small crystals. Although the data collected are marginally less precise than those collected using a monochromatic diffractometer, this is more than compensated by the speed of the data collection. The success of these and other studies has led to the construction of the new Laue diffractometer VIVALDI (Wilkinson *et al.*, 2002), which is situated permanently on a thermal-neutron beam.

References

Allen, F. H. (2002). *Acta Cryst.* B**58**, 380–388.

Allen, F. H., Kennard, O., Watson, D. G., Brammer, L., Orpen, A. G. & Taylor, R. (1992). *International Tables for Crystallography*, Vol. C, Table 9.5.1.1, pp. 685–706. Dordrecht: Kluwer Academic Publishers.

Archer, J. M. & Lehmann, M. S. (1986). *J. Appl. Cryst.* **19**, 456–458.

Barthelemy, A., Filhol, A., Rice, P. G., Allibon, J. R. & Turfat, C. (1982). *MAD*. Institut Laue–Langevin, Grenoble, France.

Brown, I. D. (1992) *Acta Cryst.* B**48**, 553–572.

Bruker (1998). *SMART and SAINT*. Bruker AXS Inc. Madison, Wisconsin, USA.
Campbell, J. W. (1995). *J. Appl. Cryst.* **28**, 228–236.
Campbell, J. W., Habash, J., Helliwell, J. R. & Moffat, K. (1996). *Q. Protein Crystallogr.* **18**, 23–31.
Cipriani, F., Castagna, J.-C., Wilkinson, C., Oleinek, P. & Lehmann, M. S. (1994). *J. Neutron Res*, **4**, 79–85.
Cleland, W. W. & Kreevoy, M. M. (1994). *Science*, **264**, 1887–1890.
Cole, J. M., McIntyre, G. J., Lehmann, M. S., Myles, D. A. A., Wilkinson, C. & Howard, J. A. K. (2001). *Acta Cryst.* A**57**, 429–434.
Filhol, A. (1998). *RAFD*19. Institut Laue–Langevin, Grenoble, France.
Goeta, A. E., Thompson, L. K., Sheppard, C. L., Tandon, S. S., Lehmann, C. W., Cosier, J., Webster, C. & Howard, J. A. K. (1999). *Acta Cryst.* C**55**, 1243–1246.
Hibbert, F. & Emsley, J. (1990). *Adv. Phys. Org. Chem.* **26**, 265–379.
Jeffrey, G. A. (1997). *Introduction to Hydrogen Bonding*. Oxford University Press.
Lough, A. J., Wheatley, P. S., Ferguson, G. & Glidewell, C. (2000). *Acta Cryst.* B**56**, 261–272.
Matthewman, J. W., Thompson, P. & Brown, P. J. (1982). *J. Appl. Cryst.* **15**, 167–173.
Myles, D. A. A., Bon, C., Langan, P., Cipriani, F., Castagna, J. C., Lehmann, M. S. & Wilkinson, C. (1998). *Physica B*, **241–243**, 1122–1130.
Pedireddi, V. R., Chatterjee, S., Ranganathan, A. & Rao, C. N. R. (1998). *Tetrahedron*, **54**, 9457–9474.
Reetz, M. T., Höger, S. & Harms, K. (1994). *Angew. Chem. Int. Ed.* **35**, 1021–1023.
Sears, V. F. (1992). *Neutron News*, **3**, 26–37.
Shan, N., Bond, A. D. & Jones, W. (2002). *Cryst. Engng*, **5**, 9–24.
Sheldrick, G. M. (1990). *Acta Cryst.* A**46**, 467–473.
Sheldrick, G. M. (1997). *SHELXL*97. University of Göttingen, Germany.
Sheldrick, G. M. (1999). *SHELXTL/PC*. Version 5.10 for Windows NT. Bruker AXS Inc. Madison, Wisconsin, USA.
Spek, A. L. (1990). *Acta Cryst.* A**46**, C-34.
Steiner, T. (1998). *J. Phys. Chem. A*, **102**, 7041–7052.
Steiner, T., Majerz, I. & Wilson, C. C. (2001). *Angew. Chem. Int. Ed.* **40**, 2651–2654.
Steiner, T., Wilson, C. C. & Majerz, I. (2000). *Chem. Commun.* pp. 1231–1232.
Thomas, M., Stansfield, R. F. D., Berneron, M., Filhol, A., Greenwood, G., Jacobé, J., Feltin, D. & Mason, S. A. (1983). *Position-Sensitive Dectection of Thermal Neutrons*, edited by P. Convert & J. B. Forsyth, pp. 344–350. New York: Academic Press.
Wilkinson, C., Cowan, J. A., Myles, D. A. A., Cipriani, F. & McIntyre, G. J. (2002). *Neutron News*, **13**, 37–41.
Wilkinson, C., Khamis, H. W., Stansfield, R. F. D. & McIntyre, G. J. (1988). *J. Appl. Cryst.* **21**, 471–478.
Wilkinson, C. & Lehmann, M. S. (1991). *Nucl. Instrum. Methods A*, **310**, 3686–3690.
Wilson, C. C. (2000). *Single Crystal Neutron Diffraction from Molecular Materials*. Singapore: World Scientific Publishing.
Wilson, C. C. (2001). *Acta Cryst.* B**57**, 435–439.